

BULLETIN OF THE CHEMICAL SOCIETY OF JAPAN, VOL. 46, 3399—3406 (1973)

## Vibration-Rotation Spectrum of Methyl Fluoride. I. Analysis of $2\nu_3$ Band

Jun NAKAGAWA, Isao SUZUKI,\* Takehiko SHIMANOCHI, and Tsunetake FUJIYAMA\*\*

*Department of Chemistry, Faculty of Science, The University of Tokyo, Bunkyo-ku, Tokyo 113**\*\*Department of Chemistry, Faculty of Science, Tokyo Metropolitan University, Setagaya-ku, Tokyo 158*

(Received July 6, 1973)

The  $2\nu_3$  band of methyl fluoride has been measured with a high-resolution infrared spectrometer. The following molecular constants are obtained:  $\nu_0=2081.382$ ,  $B''=0.85172$ ,  $B'=0.82955$ ,  $(A''-A')=0.01953$ ,  $D_J''=1.95\times 10^{-6}$ ,  $D_J'=1.78\times 10^{-6}$ ,  $D_{JK}''=1.47\times 10^{-5}$  (assumed),  $D_{JK}'=1.93\times 10^{-5}$ , and  $(D_K''-D_K')=5.9\times 10^{-6}$   $\text{cm}^{-1}$ . In addition, the hot band ( $3\nu_3\leftarrow\nu_3$ ) and the isotope  $^{13}\text{CH}_3\text{F}$  band have been observed and analyzed. The cubic force constant  $k_{333}$  was also obtained from the vibration-rotation constants.

The vibration-rotation spectra of methyl fluoride have been studied by many investigators. Pickworth and Thompson<sup>1)</sup> measured  $2\nu_3$ ,  $\nu_4$ , and some other bands above  $2000\text{ cm}^{-1}$ . Smith and Mills<sup>2)</sup> studied the  $\nu_3$  and  $\nu_6$  fundamental bands with special attention to the x,y-type Coriolis interaction between the two fundamentals.<sup>2,3)</sup> Jones, Popplewell, and Thompson<sup>4)</sup> reported the analysis of the  $\nu_2$ ,  $\nu_5$ ,  $\nu_3+\nu_4$ , and  $2\nu_4$  bands together with those of  $\text{CD}_3\text{F}$ . Blass and Edwards<sup>5)</sup> and Anttila and Huhanantti<sup>6)</sup> obtained molecular constants from some combination bands with high-resolution spectrometers. The microwave studies of this molecule were reported by Gordy and his co-workers.<sup>7-11)</sup>

The  $2\nu_3$  band of methyl fluoride has been measured under high resolution ( $\Delta\nu\approx 0.04\text{ cm}^{-1}$ ) and its rotational structures have been analyzed. With this resolving power, the  $J$ -structures in the Q-branch are completely resolved. In addition, the structures due to different values of  $K$  are observed. Since this band is free from overlapping, the highly accurate molecular constants have been determined from the simultaneous analysis of P-, Q-, and R-branches. The present paper reports the result of this study. The  $2\nu_3$  band is expected to have the x,y-type Coriolis interaction with the  $\nu_3+\nu_6$  band similar to that observed between the  $\nu_3$  and  $\nu_6$  fundamentals. As pointed out by Smith and Mills,<sup>2)</sup> the effect of this interaction is much more profound in the weaker  $\nu_3+\nu_6$  band and may not be seen on the  $2\nu_3$  band. However, the precise determination of the vibration-rotation levels in the  $2\nu_3$  band is highly desirable for the analysis of the  $\nu_3+\nu_6$  band.

\* Present address: Educational Computer Center, The University of Tokyo, Bunkyo-ku, Tokyo.

1) J. Pickworth and H. W. Thompson, *Proc. Roy. Soc., Ser. A*, **222**, 443 (1954).

2) W. L. Smith and I. M. Mills, *J. Mol. Spectrosc.*, **11**, 11 (1963).

3) C. di Lauro and I. M. Mills, *ibid.*, **21**, 386 (1966).

4) E. W. Jones, R. J. L. Popplewell, and H. W. Thompson, *Proc. Roy. Soc., Ser. A*, **290**, 490 (1965).

5) W. E. Blass and T. H. Edwards, *J. Mol. Spectrosc.*, **25**, 440 (1968).

6) R. Anttila and M. Huhanantti, *Can. J. Phys.*, **46**, 2025 (1968).

7) O. R. Gilliam, H. D. Edwards, and W. Gordy, *Phys. Rev.*, **75**, 1014 (1949).

8) C. M. Johnson, R. Trambarulo, and W. Gordy, *ibid.*, **84**, 1178 (1951).

9) W. J. Thomas, J. T. Cox, and W. Gordy, *J. Chem. Phys.*, **22**, 1718 (1951).

10) R. S. Winton and W. Gordy, *Phys. Lett.*, **32A**, 219 (1970).

11) P. A. Steiner and W. Gordy, *J. Mol. Spectrosc.*, **21**, 291 (1966).

13) K. N. Rao, C. J. Humphreys, and D. H. Rank, "Wavelength Standards in the Infrared," Academic Press, New York, London (1966).

resolved into its  $J$ -components. Additional structures due to different  $K$ -values are observed.

(2) A band head is formed at high-frequency side of R-branch. The spacing of the R-branch decreases with increasing  $J$ -values; it finally reaches the edge at  $J=36$  (see Fig. 3).

(3) An anomaly of relative intensity is observed in the P- and R-branches, particularly in the R-branch. The lines at  $J=20-25$  are weak in comparison with the other lines.

(4) A number of lines due to the hot band ( $3\nu_3 \leftarrow \nu_3$ ) and the isotope  $^{13}\text{CH}_3\text{F}$  band are identified.

### Analysis of Vibration-Rotation Structures

When none of the degenerate vibrations is excited, the energy levels of the  $v$ -th vibrational state are given by the formula,

$$T_v(J, K) = G(v) + B_v J(J+1) + (A_v - B_v) K^2 - D_J^v J^2(J+1)^2 - D_{JK}^v J(J+1) K^2 - D_K^v K^4, \quad (1)$$

where  $G(v)$  is the vibrational energy,  $A_v$  and  $B_v$  are the rotational constants, and  $D_J^v$ ,  $D_{JK}^v$ , and  $D_K^v$  are the centrifugal distortion constants.

From the selection rule for a parallel band ( $\Delta K=0$ ,  $\Delta J=0, \pm 1$ ), the transition frequencies can be calculated as the differences between the energy levels of the upper and the lower states.

**Main Band ( $2\nu_3 \leftarrow 0$ ).** In the present analysis, the following assumption is made: the value of  $D_{JK}$  in the ground state is fixed to  $1.47 \times 10^{-5} \text{ cm}^{-1}$  which has been obtained from microwave study.<sup>10</sup> The transition frequencies may be written as

$$\begin{aligned} \nu(J'', K''; J', K') &= T(J', K') - T(J'', K'') \\ &= \nu_0 + B' J'(J'+1) - D_J' J'^2(J'+1)^2 \\ &\quad + [(A' - A'') - (B' - B'')] K''^2 - B'' J''(J''+1) \\ &\quad + D_J'' J''^2(J''+1)^2 - [D_{JK}' J'(J'+1) \\ &\quad - D_{JK}'' J''(J''+1)] K''^2 - (D_K' - D_K'') K''^4, \end{aligned} \quad (2)$$

where '' and ' refer to the lower and upper states respectively.

Since the  $J$ -components in the Q-branch as well as the P- and R-branches are completely resolved, the assignment of the  $J$ -value can be done without difficulty. As mentioned earlier, the complex structures due to the  $K$ -values are found in the Q-branch. Since the statistical weights of the  $K=3p$  levels are twice those of the  $K=3p \pm 1$  levels in methyl fluoride, the assignment of these  $K$ -values can be done in consideration of the statistical weight and the relation  $K \leq J$ .

In the P- and R-branches, no structures due to the  $K$ -values are observed. In these two branches, the values of  $K$  at the intensity maxima are determined with the aid of the simulated spectra. For  $^9\text{R}(8)$  branch, for example, the intensity maximum is found near  $K=3$ , and for  $^9\text{R}(5)$  it is found near  $K=2$ .

In order to obtain the molecular constants, we have applied the least-squares method to Eq. (2), using the  $K$ -values together with  $J$ . Since we cannot determine  $A''$  and  $A'$ , and  $D_K''$  and  $D_K'$  separately, eight inde-

TABLE 1. THE MOLECULAR CONSTANTS OBTAINED FROM  $2\nu_3$  BAND OF CH<sub>3</sub>F (in  $\text{cm}^{-1}$ )

	This work	Pickworth <i>et al.</i> <sup>1)</sup>	Winton <i>et al.</i> <sup>10)</sup>
$\nu_0$	2081.382 (3) <sup>a)</sup>	2081.42	
$B''$	0.85172 (9)	0.8512	0.85179404 (5)
$B'$	0.82955 (9)	0.8289	
$(B'' - B')$	0.02217	0.0223	
$(A'' - A')$	0.01953 (11)		
$(A'' - A') - (B'' - B')$	-0.00264		
$D''$	$1.95 \times 10^{-6}$ (5)	2.2 <sub>8</sub>	1.9970 (7)
$D_J'$	$1.78 \times 10^{-6}$ (5)	2.0 <sub>2</sub>	
$D_{JK}''$	$1.47 \times 10^{-5}$ b)		1.469 (2)
$D_{JK}'$	$1.93 \times 10^{-5}$ (40)		
$(D_K'' - D_K')$	$5.9 \times 10^{-6}$ (7)		

a) The numbers in parentheses represent twice of the standard errors to be attached to the last significant figures.

b) Assumed (see text).

pendent parameters may be obtained from the observed data. The molecular constants obtained from the present study are listed in Table 1 with the corresponding constants previously determined. In Table 2, the observed and calculated frequencies are listed with their assignments. The lines which are not fully resolved are given zero or smaller weights. The standard deviation of the data is  $0.007 \text{ cm}^{-1}$ .

**Hot Band ( $3\nu_3 \leftarrow \nu_3$ ) and Isotope Band.** Two additional series of the P- and R-branches are observed between the lines of the main band, which can be assigned as the hot band ( $3\nu_3 \leftarrow \nu_3$ ) and the isotope ( $^{13}\text{CH}_3\text{F}$ ) band (see Fig. 4). The intensity ratio is expected to be 1.1:1.3:100 for the isotope band, the hot band, and the main band respectively. We may assign the stronger series as hot band and the weaker series as isotope band. As the Q-branch heads of these two series are found near 2049.7 and 2039.6  $\text{cm}^{-1}$ , the  $J$ -values in these series can be assigned. Recently the  $2\nu_3$  band of  $^{13}\text{CH}_3\text{F}$  was measured by Duncan *et al.*<sup>14</sup> with 60% enriched sample, and their results confirm the present assignment. Since the

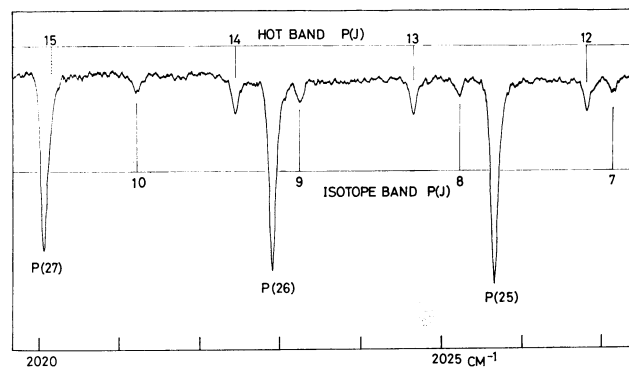


Fig. 4. The hot band and the isotope band of CH<sub>3</sub>F. Path length=6 m. Pressure=5 mmHg. Resolution=0.08  $\text{cm}^{-1}$ .

14) J. L. Duncan, D. C. McKean, and G. K. Speirs, *Mol. Phys.*, **24**, 553 (1972).

TABLE 2. OBSERVED AND CALCULATED FREQUENCIES OF  $2\nu_3$  BAND OF  $\text{CH}_3\text{F}$ 

	<i>J</i>	<i>K</i>	<i>L</i>	$\nu_{\text{obsd}}$	$\nu_{\text{calcd}}$	DIF	DIFW	Weight
QR	43	3	0	—	2112.390	—	—	0.000
QR	42	3	0	—	2112.627	—	—	0.000
QR	41	3	0	—	2112.821	—	—	0.000
QR	40	3	0	—	2112.972	—	—	0.000
QR	39	3	0	—	2113.081	—	—	0.000
QR	38	3	0	—	2113.146	—	—	0.000
QR	37	3	0	—	2113.169	—	—	0.000
QR	36	3	0	2113.159	2113.148	0.010	0.010	1.000
QR	35	3	0	2113.095	2113.085	0.010	0.010	1.000
QR	34	3	0	2112.984	2112.978	0.007	0.007	1.000
QR	33	3	0	2112.827	2112.827	−0.000	−0.000	1.000
QR	32	3	0	2112.637	2112.633	0.004	0.004	1.000
QR	31	3	0	2112.394	2112.395	−0.002	−0.002	1.000
QR	30	3	0	2112.107	2112.114	−0.006	−0.006	1.000
QR	29	3	0	2111.778	2111.789	−0.010	−0.010	1.000
QR	28	3	0	2111.415	2111.420	−0.004	−0.004	1.000
QR	27	3	0	2110.996	2111.007	−0.011	−0.011	1.000
QR	26	3	0	2110.527	2110.549	−0.022	−0.022	1.000
QR	25	3	0	2110.029	2110.048	−0.019	−0.019	1.000
QR	24	3	0	2109.488	2109.503	−0.014	−0.014	1.000
QR	23	3	0	2108.907	2108.913	−0.006	−0.006	1.000
QR	22	3	0	2108.277	2108.279	−0.002	−0.002	1.000
QR	21	3	0	2107.606	2107.601	0.005	0.005	1.000
QR	20	3	0	2106.880	2106.878	0.002	0.002	1.000
QR	19	3	0	2106.120	2106.111	0.009	0.009	1.000
QR	18	3	0	2105.305	2105.300	0.005	0.005	1.000
QR	17	3	0	2104.450	2104.444	0.007	0.007	1.000
QR	16	3	0	2103.551	2103.543	0.008	0.008	1.000
QR	15	3	0	2102.612	2102.598	0.014	0.014	1.000
QR	14	3	0	2101.619	2101.608	0.012	0.012	1.000
QR	13	3	0	2100.576	2100.573	0.003	0.003	1.000
QR	12	3	0	2099.504	2099.494	0.010	0.010	1.000
QR	11	3	0	2098.370	2098.371	−0.001	−0.001	1.000
QR	10	3	0	2097.208	2097.202	0.006	0.006	1.000
QR	9	3	0	2096.005	2095.989	0.015	0.015	1.000
QR	8	3	0	2094.732	2094.732	0.000	0.000	1.000
QR	7	2	0	2093.432	2093.419	0.013	0.013	1.000
QR	6	2	0	2092.070	2092.071	−0.001	−0.001	1.000
QR	5	2	0	2090.677	2090.679	−0.002	−0.002	1.000
QR	4	2	0	2089.236	2089.243	−0.007	−0.007	1.000
QR	3	1	0	2087.758	2087.754	0.004	0.004	1.000
QR	2	1	0	2086.232	2086.228	0.004	0.004	1.000
QR	1	0	0	2084.657	2084.656	0.001	0.001	1.000
QR	0	0	0	2083.042	2083.041	0.001	0.001	1.000
QP	1	0	0	2079.675	2079.678	−0.003	−0.003	1.000
QP	2	0	0	2077.942	2077.931	0.012	0.012	1.000
QP	3	1	0	2076.142	2076.141	0.000	0.000	1.000
QP	4	1	0	2074.312	2074.305	0.007	0.007	1.000
QP	5	2	0	2072.428	2072.433	−0.005	−0.005	1.000
QP	6	2	0	2070.507	2070.509	−0.002	−0.002	1.000
QP	7	2	0	2068.543	2068.541	0.002	0.002	1.000
QP	8	2	0	2066.528	2066.528	0.000	0.000	1.000
QP	9	3	0	2064.477	2064.485	−0.008	−0.008	1.000
QP	10	3	0	2062.374	2062.385	−0.011	−0.011	1.000
QP	11	3	0	2060.232	2060.241	−0.009	−0.009	1.000
QP	12	3	0	2058.054	2058.053	0.000	0.000	1.000
QP	13	3	0	2055.814	2055.822	−0.008	−0.008	1.000
QP	14	3	0	2053.538	2053.547	−0.009	−0.009	1.000
QP	15	3	0	2051.231	2051.229	0.001	0.001	1.000
QP	16	3	0	2048.878	2048.868	0.010	0.010	1.000

Table 2. (Continued)

	<i>J</i>	<i>K</i>	<i>L</i>	$\nu_{\text{obsd}}$	$\nu_{\text{calcd}}$	DIF	DIFW	Weight
Q P	17	3	0	2046.464	2046.463	0.000	0.000	1.000
Q P	18	3	0	2044.019	2044.016	0.003	0.003	1.000
Q P	19	3	0	2041.527	2041.525	0.001	0.001	1.000
Q P	20	3	0	2038.995	2038.992	0.003	0.003	1.000
Q P	21	3	0	2036.411	2036.416	-0.005	-0.005	1.000
Q P	22	3	0	2033.792	2033.797	-0.005	-0.005	1.000
Q P	23	3	0	2031.143	2031.137	0.006	0.006	1.000
Q P	24	3	0	2028.437	2028.433	0.004	0.004	1.000
Q P	25	3	0	2025.695	2025.688	0.007	0.007	1.000
Q P	26	3	0	2022.905	2022.900	0.004	0.004	1.000
Q P	27	3	0	2020.069	2020.071	-0.002	-0.002	1.000
Q P	28	3	0	2017.208	2017.200	0.007	0.007	1.000
Q P	29	3	0	2014.299	2014.288	0.011	0.011	1.000
Q P	30	3	0	2011.337	2011.334	0.003	0.003	1.000
Q P	31	3	0	2008.352	2008.339	0.013	0.013	1.000
Q P	32	3	0	2005.300	2005.303	-0.003	-0.003	1.000
Q P	33	3	0	2002.215	2002.226	-0.011	-0.011	1.000
Q P	34	3	0	1999.100	1999.108	-0.008	-0.008	1.000
Q P	35	3	0	1995.945	1995.950	-0.005	-0.005	1.000
Q P	36	3	0	1992.747	1992.752	-0.005	-0.005	1.000
Q Q	1	1	0	2081.335	2081.340	-0.005	-0.005	1.000
Q Q	2	2	0	2081.253	2081.259	-0.006	-0.006	1.000
Q Q	3	3	0	2081.126	2081.140	-0.013	-0.013	1.000
Q Q	4	3	0	2080.949	2080.962	-0.013	-0.009	0.500
Q Q	5	3	0	2080.739	2080.740	-0.001	-0.001	0.500
Q Q	6	6	0	2080.521	2080.547	-0.025	-0.018	0.500
Q Q	6	4	0	2080.480	2080.492	-0.012	-0.008	0.500
Q Q	7	7	0	2080.266	2080.272	-0.006	-0.004	0.500
Q Q	7	6	0	2080.230	2080.234	-0.004	-0.003	0.500
Q Q	7	4	0	2080.166	2080.181	-0.015	0.000	0.000
Q Q	8	8	0	2079.955	2079.958	-0.003	-0.003	1.000
Q Q	8	7	0	2079.906	2079.914	-0.007	-0.005	0.500
Q Q	8	6	0	2079.868	2079.877	-0.009	0.000	0.000
Q Q	8	4	0	2079.820	2079.825	-0.005	0.000	0.000
Q Q	9	9	0	2079.608	2079.606	0.002	0.002	1.000
Q Q	9	8	0	2079.555	2079.554	0.001	0.001	1.000
Q Q	9	7	0	2079.509	2079.511	-0.002	-0.002	1.000
Q Q	9	6	0	2079.472	2079.476	-0.004	-0.004	1.000
Q Q	9	4	0	2079.415	2079.425	-0.010	0.000	0.000
Q Q	10	10	0	2079.223	2079.217	0.006	0.006	1.000
Q Q	10	9	0	2079.158	2079.156	0.002	0.002	1.000
Q Q	10	8	0	2079.109	2079.106	0.003	0.003	1.000
Q Q	10	7	0	2079.063	2079.064	-0.001	-0.001	0.500
Q Q	10	6	0	2079.032	2079.030	0.002	0.001	0.500
Q Q	10	4	0	2078.965	2078.981	-0.016	0.000	0.000
Q Q	11	11	0	2078.795	2078.790	0.005	0.005	1.000
Q Q	11	10	0	2078.714	2078.720	-0.006	-0.006	1.000
Q Q	11	9	0	2078.659	2078.661	-0.002	-0.002	1.000
Q Q	11	8	0	2078.610	2078.613	-0.002	-0.002	0.500
Q Q	11	6	0	2078.533	2078.540	-0.007	0.000	0.000
Q Q	11	4	0	2078.480	2078.493	-0.013	0.000	0.000
Q Q	12	12	0	2078.330	2078.325	0.005	0.005	1.000
Q Q	12	11	0	2078.251	2078.245	0.006	0.006	1.000
Q Q	12	10	0	2078.179	2078.178	0.001	0.001	1.000
Q Q	12	9	0	2078.124	2078.122	0.003	0.003	1.000
Q Q	12	8	0	2078.076	2078.075	0.002	0.002	1.000
Q Q	12	7	0	2078.035	2078.036	-0.001	-0.001	0.500
Q Q	12	6	0	2078.000	2078.005	-0.005	-0.004	0.500
Q Q	13	13	0	2077.828	2077.823	0.004	0.003	0.500
Q Q	13	12	0	2077.736	2077.733	0.004	0.004	1.000

Table 2. (Continued)

	<i>J</i>	<i>K</i>	<i>L</i>	<i>ν</i> <sub>obsd</sub>	<i>ν</i> <sub>calcd</sub>	DIF	DIFW	Weight
QQ	13	11	0	2077.659	2077.656	0.003	0.003	1.000
QQ	13	10	0	2077.599	2077.591	0.008	0.008	1.000
QQ	13	9	0	2077.539	2077.537	0.002	0.002	1.000
QQ	13	8	0	2077.492	2077.492	−0.000	−0.000	0.500
QQ	13	6	0	2077.421	2077.426	−0.005	−0.003	0.500
QQ	13	4	0	2077.374	2077.384	−0.010	0.000	0.000
QQ	14	14	0	2077.274	2077.285	−0.012	0.000	0.000
QQ	14	13	0	2077.178	2077.183	−0.005	−0.005	1.000
QQ	14	12	0	2077.094	2077.095	−0.001	−0.001	1.000
QQ	14	11	0	2077.024	2077.022	0.003	0.003	1.000
QQ	14	10	0	2076.960	2076.960	0.001	0.001	1.000
QQ	14	9	0	2076.909	2076.908	0.001	0.001	1.000
QQ	14	6	0	2076.807	2076.802	0.004	0.003	0.500
QQ	14	4	0	2076.760	2076.763	−0.003	0.000	0.000
QQ	15	13	0	2076.494	2076.497	−0.003	−0.003	1.000
QQ	15	12	0	2076.405	2076.413	−0.008	−0.008	1.000
QQ	15	11	0	2076.338	2076.342	−0.004	−0.004	1.000
QQ	15	10	0	2076.275	2076.283	−0.008	−0.008	1.000
QQ	15	9	0	2076.229	2076.234	−0.005	−0.005	1.000
QQ	16	12	0	2075.684	2075.685	−0.001	−0.001	1.000
QQ	16	6	0	2075.423	2075.423	0.000	0.000	0.500
QQ	16	4	0	2075.387	2075.390	−0.002	0.000	0.000
QQ	17	9	0	2074.751	2074.753	−0.001	−0.001	0.500
QQ	17	6	0	2074.660	2074.667	−0.008	0.000	0.000
QQ	18	9	0	2073.947	2073.945	0.002	0.002	0.500
QQ	18	6	0	2073.867	2073.867	0.000	0.000	0.500
QQ	19	6	0	2073.026	2073.024	0.003	0.002	0.500
QQ	20	6	0	2072.130	2072.136	−0.005	−0.004	0.500
QQ	21	6	0	2071.206	2071.204	0.002	0.001	0.500
QQ	22	6	0	2070.236	2070.229	0.007	0.005	0.500
QQ	23	6	0	2069.215	2069.210	0.005	0.004	0.500
QQ	24	6	0	2068.157	2068.148	0.009	0.006	0.500
QQ	25	6	0	2067.046	2067.042	0.004	0.003	0.500
QQ	26	6	0	2065.898	2065.893	0.005	0.003	0.500

Q-branch lines in the hot band and the isotope band are too weak to be analyzed and none of the structures due to different values of *K* are resolved, the following equation is used for the transition frequencies,

$$\nu_m^{P,R} = \nu_0 + (B' + B'')m + (B' - B'' - D_{J'} + D_{J''})m^2 - 2(D_{J'} + D_{J''})m^3 - (D_{J'} - D_{J''})m^4, \quad (3)$$

TABLE 3. THE MOLECULAR CONSTANTS OBTAINED FROM (3*ν*<sub>3</sub>←*ν*<sub>3</sub>) BAND OF CH<sub>3</sub>F (in cm<sup>−1</sup>)

	This work	Smith <i>et al.</i> <sup>2)</sup>
$\nu_0 + \{(A' - A'') - (B' - B'')\} \times K^2 - (D_{K'} - D_{K'')K^4}$	2049.835 (5) <sup>a)</sup>	
<i>ν</i> <sub>0</sub>	2049.811	
<i>B</i> ''− <i>D</i> <sub><i>J</i><i>K</i></sub> '' <i>K</i> <sup>2</sup>	0.84035 (16)	0.8401
<i>B</i> ''	0.84048	
<i>B</i> '− <i>D</i> <sub><i>J</i><i>K</i></sub> ' <i>K</i> <sup>2</sup>	0.81896 (16)	
<i>B</i> '	0.81913	
( <i>B</i> ''− <i>B</i> ')	0.02135 (4)	
<i>D</i> <sub><i>J</i></sub> ''	1.93×10 <sup>−6</sup> (21)	1.86
<i>D</i> <sub><i>J</i></sub> '	1.82×10 <sup>−6</sup> (21)	
( <i>D</i> <sub><i>J</i></sub> ''− <i>D</i> <sub><i>J</i></sub> ')	0.11×10 <sup>−6</sup> (6)	

a) The numbers in parentheses represent twice of the standard errors to be attached to the last significant figures.

where *m* equals to *J*+1 for R-branch and −*J* for P-branch.

The least-squares method was applied to Eq. (3), and the following equations were obtained.

TABLE 4. THE MOLECULAR CONSTANTS OBTAINED FROM 2*ν*<sub>3</sub> BAND OF ISOTOPE <sup>13</sup>CH<sub>3</sub>F (in cm<sup>−1</sup>)

	This work	Duncan <i>et al.</i> <sup>14)</sup>	Gilliam <i>et al.</i> <sup>7)</sup>
$\nu_0 + \{(A' - A'') - (B' - B'')\}K^2 - (D_{K'} - D_{K'')K^4}$	2039.680 (11) <sup>a)</sup>	2039.68	
<i>ν</i> <sub>0</sub>	2039.656		
<i>B</i> ''− <i>D</i> <sub><i>J</i><i>K</i></sub> '' <i>K</i> <sup>2</sup>	0.82892 (36)	0.8305	
<i>B</i> ''	0.82906		0.82932
<i>B</i> '− <i>D</i> <sub><i>J</i><i>K</i></sub> ' <i>K</i> <sup>2</sup>	0.80794 (36)	0.8093	
<i>B</i> '	0.80811		
( <i>B</i> ''− <i>B</i> ')	0.02095 (11)	0.02099	
<i>D</i> <sub><i>J</i></sub> ''	1.79×10 <sup>−6</sup> (50)	2.2	
<i>D</i> <sub><i>J</i></sub> '	1.81×10 <sup>−6</sup> (50)		
( <i>D</i> <sub><i>J</i></sub> ''− <i>D</i> <sub><i>J</i></sub> ')	−0.02×10 <sup>−6</sup> (22)		

a) The numbers in parentheses represent twice of the standard errors to be attached to the last significant figures.

TABLE 5. OBSERVED FREQUENCIES OF ( $3\nu_3 \leftarrow \nu_3$ ) BAND OF CH<sub>3</sub>F AND  $2\nu_3$  BAND OF <sup>13</sup>CH<sub>3</sub>F

<i>J</i>	$(3\nu_3 \leftarrow \nu_3)$ of CH <sub>3</sub> F				$2\nu_3$ of <sup>13</sup> CH <sub>3</sub> F			
	R-Branch		P-Branch		R-Branch		P-Branch	
	Obsd	$\Delta\nu^a$	Obsd	$\Delta\nu^a$	Obsd	$\Delta\nu^a$	Obsd	$\Delta\nu^a$
0	—				—			
1	—		—		—		—	
2	—		—		—		—	
3	2056.117	12	—		—		—	
4	57.595	0	2042.860	4	2047.347	9	2032.776	-21
5	59.012	-7	41.004	0	—		—	
6	—		—		50.103	-4	29.087	-18
7	61.737	0	37.180	6	—		27.205	9
8	63.029	-2	35.196	2	52.709	3	25.254	8
9	64.284	2	33.172	-2	53.958	15	23.249	-4
10	65.490	0	—		55.141	4	21.231	12
11	—		29.014	9	56.273	-15	19.144	-1
12	67.787	16	26.859	1	57.405	8	17.030	3
13	68.851	-5	24.666	-2	58.453	-10	14.863	-6
14	69.899	8	22.443	7	59.481	-5	12.677	7
15	70.886	2	—		—		10.435	6
16	71.824	-9	17.839	-8	61.420	15	08.165	19
17	72.738	-1	15.487	-3	—		05.821	-1
18	73.601	-1	13.092	0	63.150	-4	03.443	-14
19	74.434	12	10.652	1	63.946	-17	01.039	-12
20	75.204	5	08.165	-5	—		1998.593	-10
21	75.936	4	05.645	-2	—		—	
22	76.610	-13	03.082	0	66.143	9	93.596	12
23			00.473	-4				
24			1997.830	-1				
25			95.141	-2				
26			92.423	8				

a) (observed frequency—calculated frequency)  $\times 1000 \text{ cm}^{-1}$ 

$$\nu_m^{\text{P,R}} = 2049.835 + 1.65932m - 0.021392m^2 \\ - 7.51 \times 10^{-6}m^3 + 1.13 \times 10^{-7}m^4, \\ \text{(for hot band)}$$

$$\nu_m^{\text{P,R}} = 2039.680 + 1.63687m - 0.020983m^2 \\ - 7.17 \times 10^{-6}m^3 - 0.21 \times 10^{-7}m^4. \\ \text{(for isotope band)} \quad (4)$$

These constants include the contributions from the  $K^2$  and  $K^4$  terms, because the  $K$ -values at the intensity maxima are not equal to zero. If we assume  $K=3$  at the intensity maxima and the values  $[(A'-A'')-(B'-B'')]$ ,  $D_{JK''}$ ,  $D_{JK'}$ , and  $(D_{K'}-D_{K''})$  to be the same as those of main band, we can estimate the 'true' molecular constants. In Tables 3 and 4, the molecular constants which were corrected for the  $K$ -dependent terms are tabulated together with the corresponding constants obtained by Smith and Mills,<sup>2)</sup> by Duncan *et al.*,<sup>14)</sup> and by Gilliam and Gordy.<sup>7)</sup> In Table 5, the observed and calculated frequencies are listed. The standard deviations of these data are  $0.008 \text{ cm}^{-1}$  for the hot band and  $0.012 \text{ cm}^{-1}$  for the isotope band.

### Discussion

The molecular constants given in Table 1 have been obtained from the simultaneous analysis of 135 transi-

tions in the P-, Q-, and R-branches. Their values, particularly those for  $\nu_0$ ,  $(B'-B'')$ , and  $(D'-D'')$ , are determined very accurately. This is also the first case, as far as we know, in which the  $(A'-A'')$  value is obtained for the parallel band of methyl fluoride. From the analysis of the  $\nu_3$  fundamental band, Smith and Mills<sup>2)</sup> estimate  $|(A'-A'')-(B'-B'')| = |\alpha_3^A - \alpha_3^B| = 0.0002 \text{ cm}^{-1}$ . Our present result ( $0.0013 \text{ cm}^{-1}$ ) is one order of magnitude larger than their estimation, but quite close to the value recently obtained from laser spectroscopy ( $0.0011 \text{ cm}^{-1}$ ).<sup>15)</sup>

For the hot band and isotope band, the number of observed lines is not enough to determine the centrifugal distortion constants with high accuracy. The standard errors of these constants are comparatively larger than the other ones.

In the  $2\nu_3$  band the  $(B''-B')$  value is fairly large in comparison with  $(B''+B')$ , which makes the R-branch to have a distinct band head. If the centrifugal distortion terms and the  $K$ -dependent terms in Eq. (2) are neglected, the following expression quadratic to  $J$  is obtained for R-branch.

$$\nu(J; J+1) = \nu_0 + (B''+B')(J+1) - (B''-B')(J+1)^2, \quad (5)$$

which has a maximum at  $J = [(B''+B')/2(B''-B')] - 1 = 37$ .

15) T. Y. Chang and J. D. McGee, *Appl. Phys. Lett.*, **19**, 103 (1971).

The rotational constants of  $v$ -th vibrational state can be expressed as,

$$B_v = B_e - \sum_s \alpha_s^B (v_s + d_s/2) + \sum_s \sum_{s'} \gamma_{ss'}^B (v_s + d_s/2)(v_{s'} + d_{s'}/2) + \dots \quad (6)$$

where  $B_e$  is the equilibrium rotational constant,  $\alpha_s^B$  and  $\gamma_{ss'}^B$  are the vibration-rotation constants, and  $d_s$  is the degree of the degeneracy. From the analysis of  $\nu_3$  fundamental band,<sup>2)</sup> the value of  $\alpha_3^B = (B'' - B')$  was given as  $0.01134 (\pm 3) \text{ cm}^{-1}$ . The present results yield  $0.01180 \text{ cm}^{-1}$  for  $\alpha_3^B$  and  $0.00023 \text{ cm}^{-1}$  for  $\gamma_{33}^B$ .

The vibration-rotation constants,  $\alpha_3^B$  and  $\alpha_3^A$  can be written as the sum of the harmonic and anharmonic parts.<sup>16,17)</sup>

$$\begin{aligned} \alpha_3^B &= \alpha_3^B(\text{harm}) + \alpha_3^B(\text{anharm}), \\ \alpha_3^B(\text{harm}) &= -(2B_e^2/\omega_3)[3A_{33}^{xx} + 4\{(\zeta_{34}^{xx}\omega_4)^2/(\omega_3^2 - \omega_4^2) \\ &\quad + (\zeta_{35}^{xx}\omega_5)^2/(\omega_3^2 - \omega_5^2) + (\zeta_{36}^{xx}\omega_6)^2/(\omega_3^2 - \omega_6^2)\}], \\ \alpha_3^B(\text{anharm}) &= -4\pi B_e^2(c/h)^{1/2}\{3a_3^{xx}k_{333}/\omega_3^{3/2} \\ &\quad + a_1^{xx}k_{133}/\omega_1^{3/2} + a_2^{xx}k_{233}/\omega_2^{3/2}\}, \end{aligned} \quad (7)$$

$$\begin{aligned} \alpha_3^A &= \alpha_3^A(\text{harm}) + \alpha_3^A(\text{anharm}), \\ \alpha_3^A(\text{harm}) &= -6A_e^2A_{33}^{zz}/\omega_3 \\ \alpha_3^A(\text{anharm}) &= -4\pi A_e^2(c/h)^{1/2}\{3a_3^{zz}k_{333}/\omega_3^{3/2} \\ &\quad + a_1^{zz}k_{133}/\omega_1^{3/2} + a_2^{zz}k_{233}/\omega_2^{3/2}\}, \end{aligned} \quad (8)$$

in which  $a_s^{aa}$  and  $A_{ss}^{aa}$  are related, respectively, to the first and the second derivatives of moment of inertia  $I_{aa}$ , expanded in normal coordinate  $Q_s$ .  $\zeta_{ss'}^a$  is the Coriolis coupling constant.

If the harmonic force field is known, the constants which appear in Eqs. (7) and (8) may be calculated. From the force field which was obtained in our laboratory<sup>18)</sup> the following relations are derived;

$$\begin{aligned} \alpha_3^B(\text{obsd}) &= 0.01180, \\ \alpha_3^B(\text{harm}) &= -0.00031, \\ \alpha_3^B(\text{anharm}) &= -0.000180 k_{333} - 0.000004 k_{133} \\ &\quad + 0.000005 k_{233}, \end{aligned} \quad (9)$$

and

$$\begin{aligned} \alpha_3^A(\text{obsd}) &= 0.00977, \\ \alpha_3^A(\text{harm}) &= -0.0009, \\ \alpha_3^A(\text{anharm}) &= +0.000070 k_{333} - 0.000189 k_{133} \\ &\quad + 0.000242 k_{233}. \end{aligned} \quad (10)$$

Since both  $\alpha_3^B(\text{harm})$  and  $\alpha_3^A(\text{harm})$  are found relatively small and have opposite signs to the  $\alpha_3^B(\text{obsd})$  and  $\alpha_3^A(\text{obsd})$ , the anharmonic parts  $\alpha_3^B(\text{anharm})$  seem to have a predominant role. Although

three cubic force constants are involved in the expression, the coefficient of  $k_{333}$  is about 40 times larger than the other two in Eq. (9). Therefore, if we consider the cubic diagonal force constant  $k_{333}$  only, we could have  $-67 \text{ cm}^{-1}$  for  $k_{333}$ . The three coefficients in Eq. (10) are of the same order and we cannot determine the other two cubic force constants.

TABLE 6. COMPARISON BETWEEN THE  $\nu_3$  OF  $\text{CH}_3\text{F}$  AND DIATOMIC C-F MOLECULE (in  $\text{cm}^{-1}$ )

	$\text{CH}_3\text{F}$		C-F <sup>19)</sup>
$\nu_3$	1048.60 <sup>2)</sup>	$\nu$	1286.26
$2\nu_3$	2081.38	$2\nu$	2550.99
$3\nu_3$	3098.42	$3\nu$	3794.92
$\omega_3^c$	1064.37	$\omega_e$	1308.1
$x_{33}$	8.01	$\omega_e x_e$	11.10
$y_{333}$	+0.02	$\omega_e y_e$	0.093
$\alpha_3^B$	0.01180	$\alpha_e$	0.01840
$\gamma_{33}^B$	0.00023	$\gamma_e$	0.00011
$k_{333}$	-67	$k_3$	-91

A rough estimation of  $k_{333}$  may be done from the spectroscopic data of diatomic CF,<sup>19)</sup> since the normal coordinate  $Q_3$  is chiefly associated with the C-F stretching coordinate. The data which are obtained from the analysis of CF molecule are listed in Table 6 in comparison with those of the C-F stretching vibration of methyl fluoride. When we assume the Morse function for the potential of C-F stretching vibration, the following relation can be obtained,

$$k_3(\text{CF})/\omega_e(\text{CF}) = k_{333}(\text{CH}_3\text{F})/\omega_3(\text{CH}_3\text{F}). \quad (11)$$

With the aid of Eq. (11) and Table 6, the  $k_{333}$  is estimated to be  $-75 \text{ cm}^{-1}$ , which has certainly correct order of magnitude.

As mentioned earlier, the x,y-type Coriolis interaction would likely occur between the  $2\nu_3$  band and the  $\nu_3 + \nu_6$  band. The selection rule for this type of interaction is  $\Delta J=0$ ,  $\Delta k=+1$ , and  $\Delta l=+1$  or  $\Delta J=0$ ,  $\Delta k=-1$ , and  $\Delta l=-1$ ,<sup>3)</sup> where  $K=|k|$ . We have observed the combination  $\nu_3 + \nu_6$  band and made a preliminary analysis. From the molecular constants so far available, we can predict that the interaction would be strong at relatively high  $K$  levels ( $K \sim 25$ ).

The intensity anomaly due to the Coriolis interaction will be seen more clearly in the weaker  $\nu_3 + \nu_6$  band. The more precise analysis of the  $\nu_3 + \nu_6$  combination band is being attempted, the result will be published in the near future.

This research has been supported by the grant from the Ministry of Education. Helpful discussions from Dr. Koichi Yamada are deeply appreciated.

16) H. H. Nielsen, *Rev. Mod. Phys.*, **23**, 90 (1951).

17) T. Oka and Y. Morino, *J. Mol. Spectrosc.*, **6**, 472 (1961).

18) T. Shimanouchi, "The Molecular Force Field," in "Physical Chemistry," Vol. 4, p. 290, ed. by H. Eyring, D. Henderson, and W. Jost, Academic Press, New York (1970).

19) T. L. Porter, D. E. Mann, and N. Acquista, *J. Mol. Spectrosc.*, **16**, 228 (1965).